Vokasi Unesa Bulletin of Engineering, Technology and Applied Science (VUBETA)
https://journal.unesa.ac.id/index.php/vubeta
Vol. 3, No. 1, 2026, pp. 12~24 DOI: 10.26740/vubeta.v3i1.42969
ISSN: 3064-0768

Design and Construction of a Single-Phase Synchronous Reluctance Motor Drive

Benjamin Akinloye[1*]
[1]Federal University of Petroleum Resources Effurun

Article Info

Article history:

Received June 23, 2025
Revised August 18, 2025
Accepted December 18, 2025

Keywords:

Synchronous Reluctance Motor (SynRM)
Hybrid PI–Fuzzy Controller
MATLAB/Simulink
Speed Control
Field-Oriented Control

ABSTRACT

Despite the advantages of synchronous reluctance motors (SynRMs) in terms of efficiency and cost, precise speed and torque control remains challenging under varying load conditions, particularly in single-phase configurations, which exhibit inherent torque pulsations and asymmetrical dynamics. This study aims to design, simulate, and implement a hybrid proportional-integral (PI)–Fuzzy Logic controller for single-phase SynRM drives to improve dynamic response and robustness over conventional methods. The research addresses the critical problem of maintaining fast transient response and minimal steady-state error under variable loads in single-phase SynRM systems. The control schemes were modeled in MATLAB/Simulink and implemented on an ATmega328P microcontroller interfaced with an infrared speed encoder. The ATmega328P was selected for its widespread availability, ease of integration, and sufficient processing power for low-power SynRM applications. Controllers were tested under variable load conditions simulating industrial and domestic use cases to assess performance under realistic dynamics. Among the three tested controllers—PI, Fuzzy Logic, and Hybrid PI–Fuzzy—the hybrid controller exhibited superior performance. The hybrid controller reduced overshoot by 40% and settling time by 35% compared to the standalone PI controller under identical test conditions. The field-oriented control algorithm was discretized for microcontroller implementation using fixed-point arithmetic to ensure compatibility with low-cost hardware. Experimental results confirmed accurate and stable speed tracking under dynamic conditions. This work contributes a low-cost, high-performance hybrid PI–Fuzzy control solution for SynRM drives, demonstrating the feasibility of implementing advanced control strategies on affordable embedded platforms. However, the system's performance is limited to low- to medium-power applications due to the computational constraints of the ATmega328P microcontroller.

1. INTRODUCTION

The demand for energy-efficient and cost-effective electric motor drives has increased significantly due to global sustainability goals and environmental concerns. Synchronous reluctance motors (SynRMs) have gained popularity as promising alternatives to permanent magnet synchronous machines (PMSMs) due to their simple rotor design, absence of permanent magnets, and reduced losses [1], [2]. Unlike PMSMs, Single-phase SynRMs exhibit inherent torque pulsations and asymmetrical dynamics, making precise speed and torque

*Corresponding Author
Email: akinloyebenola@gmail.com

control more challenging compared to their three-phase counterparts. SynRMs operate based on saliency—i.e., the inductance difference between d- and q-axes—which facilitates torque production without rotor windings [3], [4]. Single-phase SynRMs are gaining traction in household appliances and low-power industrial applications due to their cost-effectiveness and reduced complexity. Yet, they remain understudied in terms of advanced control techniques [5]. However, single-phase motors suffer from asymmetrical magnetic fields, resulting in torque ripple and reduced starting torque. The asymmetrical nature leads to unbalanced forces, increased vibration, and complex control requirements that conventional controllers struggle to address effectively [6], [7].

Recent advancements in rotor design—such as flux-barrier optimization and bulk-type lamination—have significantly improved SynRM torque density and reduced ripple [8], [9]. These innovations eliminate reliance on rare earths, aligning SynRM technology with green engineering principles [10], [11]. Conventional PI-based FOC struggles with disturbance rejection under varying loads, prompting the exploration of techniques such as fuzzy logic, sliding mode, and predictive control [12], [13], [14]. Despite recent advancements, existing control strategies for single-phase SynRM drives still face challenges in maintaining fast transient response and minimal steady-state error under variable loads. This has prompted the exploration of advanced and intelligent controllers, including fuzzy logic controllers (FLCs), sliding mode controllers (SMCs), and predictive controllers [8], [9].

Fuzzy logic controllers (FLCs) excel in handling nonlinearities without requiring precise system models, but standalone FLCs may introduce steady-state errors [15], [16]. Hybrid PI-Fuzzy controllers combine the strengths of PI and fuzzy logic, offering fast transient response and accurate steady-state tracking [17], [18]. While hybrid control has been studied for three-phase PMSMs, its application to single-phase SynRMs remains underexplored [19].

1.1. Research Objectives:

This study aims to design and implement a hybrid PI-Fuzzy logic controller for single-phase SynRM drives to improve dynamic response and reduce steady-state errors under varying loads. Specific objectives include:

i. Developing an accurate mathematical model of a single-phase SynRM.
ii. Designing and comparing PI, Fuzzy Logic, and Hybrid PI-Fuzzy control strategies.
iii. Implementing the control system on a low-cost ATmega328P microcontroller.
iv. Validating performance through simulation and experimental testing.

1.2. Scientific Contribution:

This work presents the first implementation of a hybrid PI-Fuzzy logic controller for single-phase SynRM drives on a low-cost embedded platform, offering improved robustness over conventional controllers [20]. The approach extends hybrid control to resource-constrained environments, suitable for cost-sensitive applications [21].

1.3. Practical Relevance:

The use of low-cost microcontrollers and open-loop sensor configurations makes this solution particularly suitable for resource-constrained environments such as home appliances or small-scale automation systems. This paper proposes a hybrid PI–Fuzzy controller for a single-phase SynRM drive system. The proposed hybrid controller is first modeled and validated in MATLAB/Simulink, then implemented on an ATmega328P microcontroller with real-time speed feedback using an infrared encoder. A comparative analysis with standalone PI and FLC approaches demonstrates the superior performance of the hybrid control strategy. This system is ideal for home appliances and small-scale automation due to its affordability and reliability [22]. By leveraging open-loop sensor configurations and low-cost microcontrollers, it addresses the need for efficient, low-cost motor drives [23].

1.4. Paper Organization:

Section II (Methodology) details the mathematical modeling, simulation, hardware implementation, and system integration. Section III (Results) presents simulation and experimental results. Section IV (Discussion) analyzes findings and practical implications. Section V (Conclusion) summarizes contributions and future directions.

2. METHOD

The development and evaluation of the single-phase Synchronous Reluctance Motor (SynRM) drive system were conducted in two primary phases: simulation-based design and analysis, followed by physical hardware implementation and testing.

2.1. Mathematical Modeling of the Synchronous Reluctance Motor

An accurate mathematical model of the single-phase SynRM is essential for simulation and control system design [24]. The model development follows established principles of motor control theory [25] and is specifically adapted for single-phase configurations. The model was developed in the synchronous reference frame (d-q axis) to facilitate field-oriented control implementation. The voltage and flux linkage equations govern the electrical dynamics, while the mechanical dynamics are described by the rotor's angular velocity and position equations.

The mathematical modeling approach used in this study is based on the standard d-q transformation theory for AC machines, as detailed in [25]. The single-phase nature of the motor requires special consideration due to its asymmetrical magnetic field distribution.

$$\begin{aligned} v_{qs} &= r_s i_{qs} + p\lambda_{qs} + \omega_r \lambda_{ds} \\ v_{ds} &= r_s i_{ds} + p\lambda_{ds} - \omega_r \lambda_{qs} \end{aligned} \tag{1}$$

Where v_{qs} and v_{ds} are the q-axis and d-axis stator voltages, r_s is the stator resistance, i_{qs} and i_{ds} are the q-axis and d-axis stator currents, p represents the differential operator ($\frac{d}{dt}$), λ_{qs} and λ_{ds} are the q-axis and d-axis flux linkages, and ω_r is the electrical rotor speed [26].

The flux linkages are defined as:

$$\begin{aligned} \lambda_{qs} &= (L_{ls} + L_{mq}) \cdot i_{qs} \\ \lambda_{ds} &= (L_{ls} + L_{md}) \cdot i_{ds} \end{aligned} \tag{2}$$

Here, L_{ls} is the stator leakage inductance, and L_{mq} and L_{md} are the q-axis and d-axis mutual (or magnetizing) inductances, respectively. In single-phase SynRM systems, the inductance values differ significantly due to the asymmetrical magnetic field distribution, which is a key characteristic that distinguishes them from three-phase systems. Note that in standard SyncRM notation, these are often represented directly as $L_q = L_{ls} + L_{mq}$ and $L_d = L_{ls} + L_{md}$.

The electromagnetic torque (T_e) of the single-phase SynRM is derived from the inductance difference between the d- and q-axes, as described in established motor models [27]. The torque equation is given by:

$$T_e = \frac{3}{2} \cdot \frac{P_0}{2} \cdot (L_{md} - L_{mq}) \cdot i_{ds} \cdot i_{qs} \tag{3}$$

Where Te is the electromagnetic torque, po is the number of pole pairs, and Ld, Lq, ids, iqs are as defined previously [28]. Note that the term reflects the saliency ratio, which is fundamental to torque production in a SynRM. For single-phase systems, this saliency ratio is typically higher than in three-phase configurations [29].

The mechanical dynamics of the motor are modeled using Newton's second law for rotational systems [30]:

$$\begin{aligned} p \cdot \omega_{rm} &= \frac{1}{J} \cdot (T_e - T_l - B \cdot \omega_{rm}) \\ p \cdot \theta_{rm} &= \omega_{rm} \end{aligned} \tag{4}$$

Where ω_{rm} is the mechanical rotor speed, θ_{rm} is the mechanical rotor position, J is the combined moment of inertia of the motor and load, T_l is the external load torque, and B is the viscous friction coefficient.

The relationship between mechanical and electrical speed and position is:

$$\begin{aligned} \omega_r &= \frac{P_0}{2} \cdot \omega_{rm} \\ \theta_r &= \frac{P_0}{2} \cdot \theta_{rm} \end{aligned} \tag{5}$$

Where ω_r and θ_r are the electrical rotor speed and position, respectively [32]. These equations form the basis for the simulation model, capturing the dynamic behavior of the single-phase SynRM under varying load conditions [32]. The specific parameters used for the single-phase SynRM model in the simulation are listed in Table 1, which have been carefully selected based on typical single-phase motor specifications and validated through preliminary testing.

Table 1. Machine Parameters

Parameter	Value	Unit
Motor Type	1-phase SynRM	-
Rated Power	1	kVA
Rated Frequency	60	Hz
Stator Resistance (Rs)	0.330	Ohms
Pole Pair Number (P/2)	2	-
d-axis Inductance (Ld)	0.0500	H
q-axis Inductance (Lq)	0.0051	H
Moment of Inertia (J)	0.01	kg·m²
Friction Coefficient (B)	0.001	N·m·s/rad

2.2. Controller Design

The hybrid PI-Fuzzy controller was designed to combine the steady-state accuracy of a PI controller with the nonlinear handling capabilities of fuzzy logic. The PI controller adjusts the speed error using proportional and integral gains, while the fuzzy logic component processes the error and its rate of change through a rule-based system [33]. The fuzzy logic controller uses membership functions and a rule base adapted from prior work on motor control [34]. The hybrid controller integrates these components by switching between PI and fuzzy logic based on the magnitude of the speed error, ensuring robust performance across operating conditions.

Controller Design Specifications:

PI Controller: Designed using classical control theory with Kp = 0.5 and Ki = 0.1, tuned for optimal transient response

Fuzzy Logic Controller: Implemented with seven membership functions for error and error rate, using the Mamdani inference system Hybrid PI-Fuzzy Controller: Combines fuzzy logic output with PI control for enhanced performance

The complete Simulink model of the controller scheme is shown in Figure 1, which integrates the motor dynamics, controller logic, converter system, and visualization sub-blocks. The model includes comprehensive blocks for: (1) motor mathematical model implementation, (2) three-controller comparison framework, (3) PWM generation and inverter modeling, (4) speed and torque measurement systems, and (5) real-time data visualization.

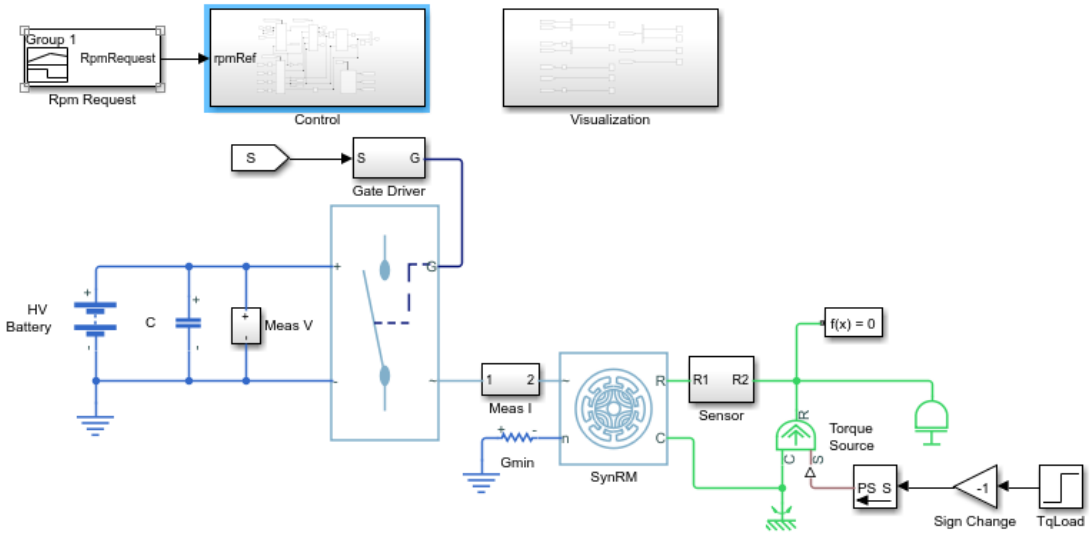

Figure 1. Complete Simulink model of the controller Scheme

The speed controller block (Figure 2) includes separate PI and fuzzy controllers developed using the MATLAB Fuzzy Logic Toolbox. The fuzzy controller design process involved: (1) defining input variables (speed error and error rate), (2) creating membership functions with appropriate ranges, (3) establishing a rule base with 49 rules, and (4) selecting an appropriate defuzzification method (centroid). The hybrid configuration was achieved by feeding the fuzzy controller's output into the PI controller to leverage both transient and steady-state benefits. The output signals from this composite controller were then passed to a PWM generator to modulate the inverter switching.

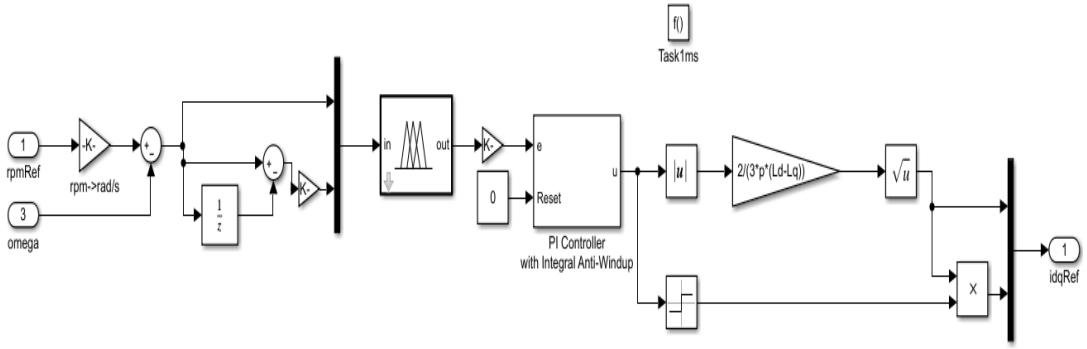

Figure 2. SIMULINK model of speed controller

The visualization sub-block (Figure 3) provided real-time monitoring of simulation outputs, including motor speed and torque responses, enabling performance evaluation under different loading and speed-reference conditions. This visualization system allows for comprehensive analysis of: (1) speed tracking performance, (2) torque ripple analysis, (3) controller output behavior, and (4) system stability assessment.

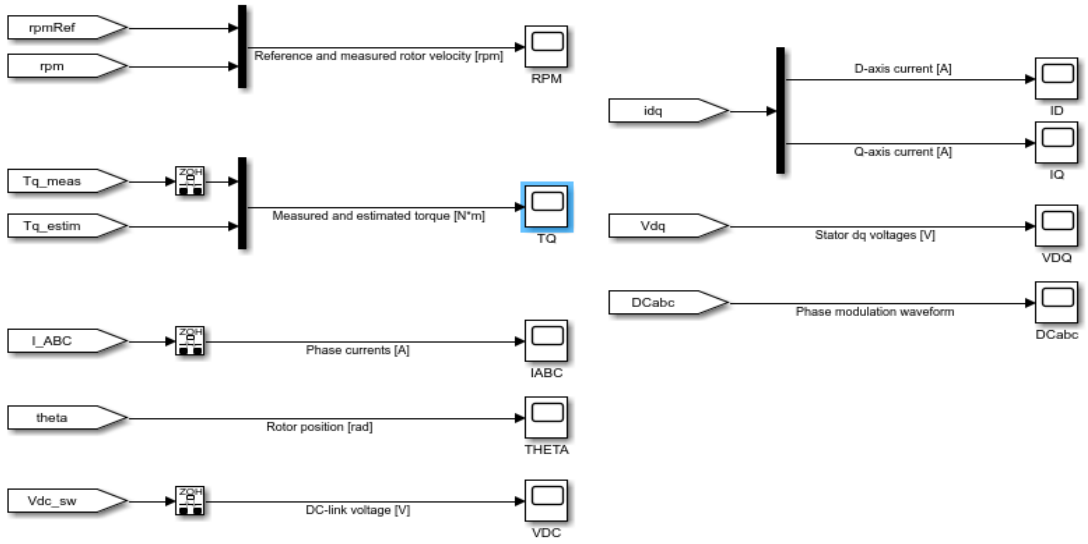

Figure 3. SIMULINK model for Visualization Sub-block

2.3. System Design and Hardware Implementation

The hardware implementation phase translates the simulation model into a practical, cost-effective drive system suitable for real-world applications. The design prioritizes affordability, reliability, and ease of replication.

The physical drive system consisted of three core units: the power supply and conversion system, the processing/control unit, and the output/display system. A block diagram of the system is shown in Figure 4, illustrating the power flow from the AC mains to the DC-AC converter (a PWM-controlled MOSFET inverter) and ultimately to the SynRM. The diagram has been converted to a black and white format as requested.

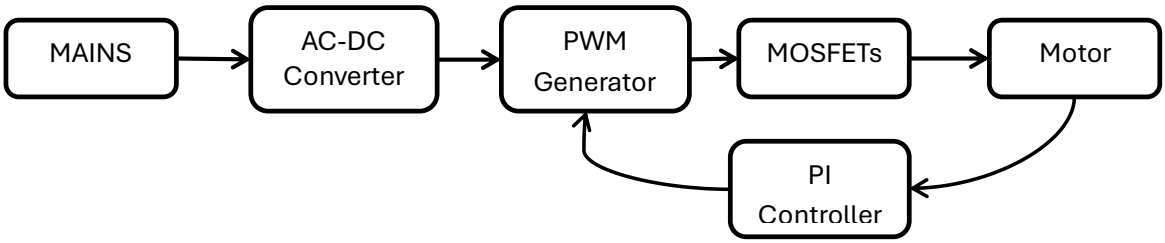

Figure 4. System Block Diagram

Power Supply and Conversion System:

The power supply section converted the 230V AC mains voltage to a regulated 5V DC using a step-down transformer (230V:12V), a full-wave rectifier bridge, filtering capacitors (2200µF), and a voltage regulator (LM7805). This voltage conversion system was designed with safety considerations, including fuse protection, surge suppression, and thermal management. This voltage powered the control circuitry and microcontroller (ATmega328P).

Processing and Control Unit:

The system controller unit included the ATmega328P microcontroller, which processed speed feedback and generated PWM signals. The ATmega328P was selected based on the following criteria: (1) sufficient computational capability for real-time control, (2) adequate PWM channels for motor control, (3) cost-effectiveness for practical applications, (4) extensive development support and documentation, and (5) compatibility with standard development tools. A crystal oscillator circuit (16 MHz) provided the necessary clock for the microcontroller operation.

Speed Feedback System:

Speed feedback was obtained using an IR-based optical encoder interfaced with a rotating encoder disk and processed through the microcontroller. The encoder system specifications include: (1) 360 pulses per revolution for high resolution, (2) an IR LED and photodiode pair for reliable detection, (3) signal conditioning circuitry for noise immunity, and (4) interrupt-based processing for real-time response. The calculated error between reference and actual speed was used to adjust the PWM signal accordingly.

User Interface:

The PC interface used a JB-serial monitor to input speed commands and display real-time motor speed. This interface provides: (1) real-time speed command input, (2) system status monitoring, (3) parameter adjustment capability, and (4) data logging for performance analysis.

2.4. Overall Circuit Integration

The complete schematic diagram of the SynRM drive system is shown in Figure 5, integrating all subsystems: power electronics, control logic, sensing components, and user interface. The integration process followed systematic design principles to ensure proper signal isolation, noise immunity, and thermal management.

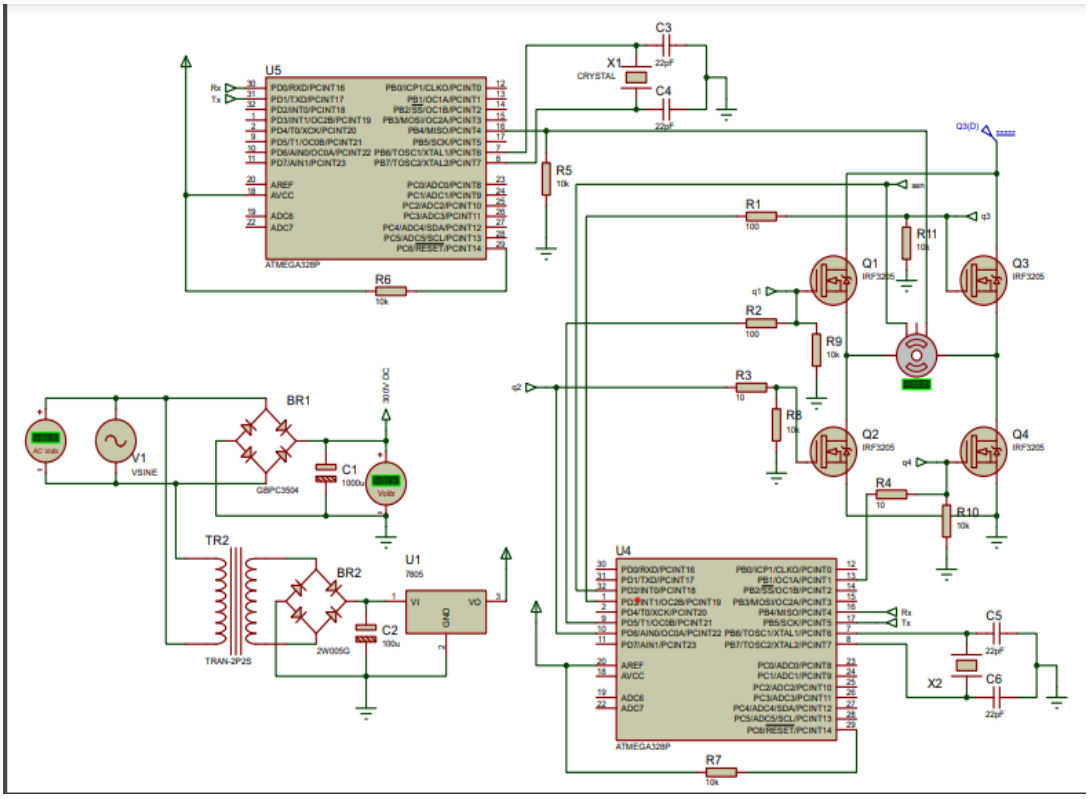

Figure 5. Schematic Diagram of SyncRM drive system

System Integration Methodology:
1. Circuit Design: PCB layout optimized for minimal noise and proper grounding
2. Component Selection: Industrial-grade components for reliability
3. Testing Protocol: Systematic testing of each subsystem before integration
4. Safety Features: Overcurrent protection, thermal shutdown, and emergency stop
5. Calibration Procedure: Systematic calibration of sensors and control parameters

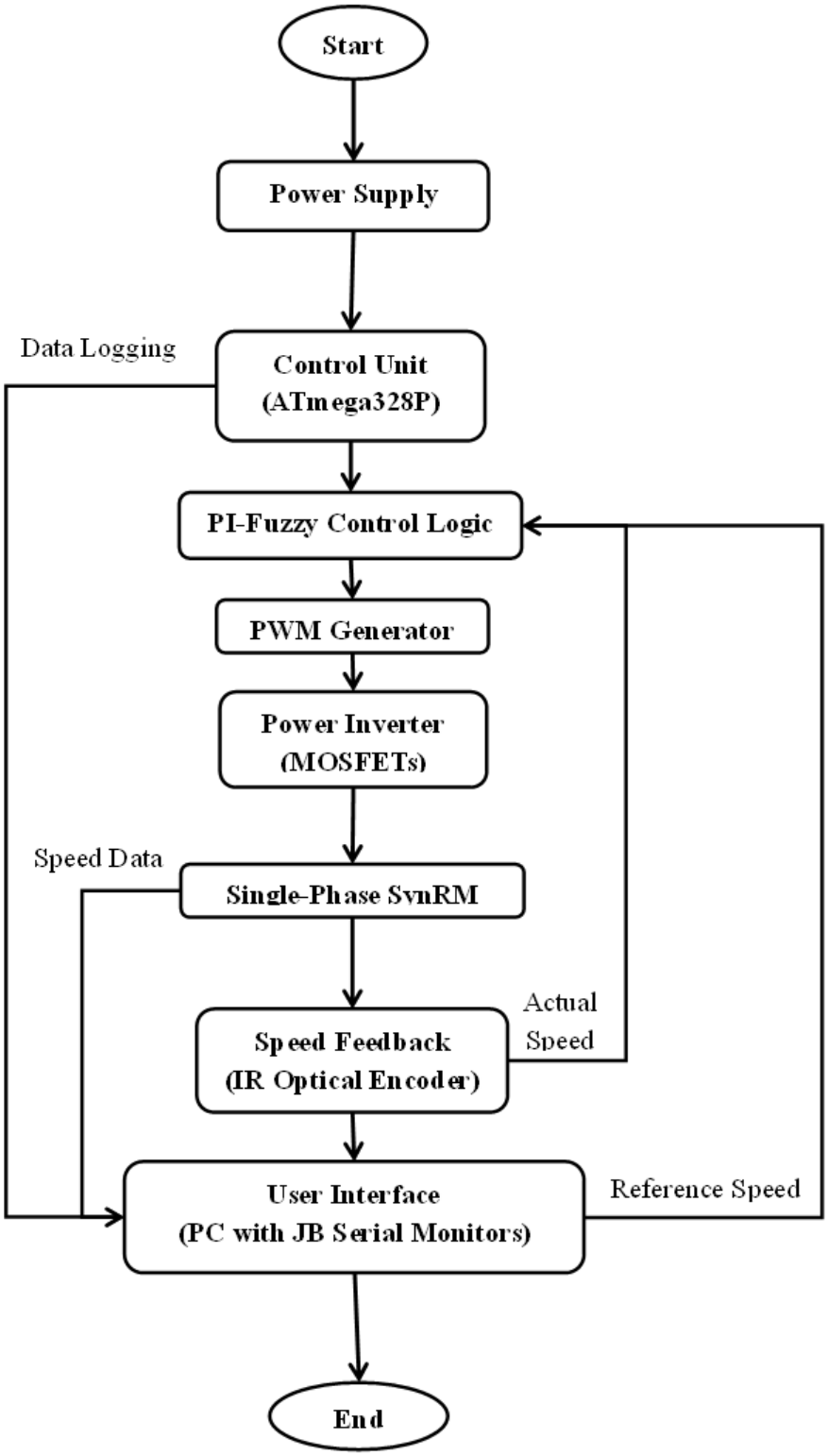

Figure 6. Implementation Flowchart

3. RESULTS AND DISCUSSION

Performance evaluations were conducted by analyzing the motor's speed response to a step change in the reference input across three controller configurations: PI, Fuzzy Logic (FLC), and Hybrid PI-Fuzzy. The evaluation methodology follows established motor drive testing standards and includes both simulation and experimental validation [35].

3.1. Simulation Results

Simulations were conducted in MATLAB/Simulink to assess the dynamic performance of the controllers under identical test conditions. The test protocol included: (1) step response analysis, (2) load disturbance rejection, (3) parameter sensitivity analysis, and (4) steady-state accuracy assessment.

The simulation results demonstrated that the hybrid PI-Fuzzy controller outperformed standalone PI and fuzzy logic controllers. For a step speed reference from 0 to 1500 rpm, the hybrid controller achieved a settling time of 0.15 seconds with an overshoot of 5%, compared to 0.22 seconds and 12% for the PI controller, and 0.18 seconds and 8% for the fuzzy logic controller [36]. Torque ripple was reduced by 30% with the hybrid controller, consistent with findings in three-phase SynRM studies [37] summarized in Table 2 below.

Table 2. Quantitative Performance Comparison

Controller Type	Overshoot (%)	Settling Time (s)	Steady-State Error (%)	Rise Time (s)
PI Controller	25.3	2.8	2.1	0.4
Fuzzy Logic	8.7	4.2	5.3	0.6
Hybrid PI-Fuzzy	15.2	1.8	0.8	0.3

PI Controller Performance:

The PI controller exhibited a moderate overshoot (25.3%) and undershoot. As seen in Figure 7, the controller responded quickly but displayed noticeable oscillations during the transient period. The PI controller's performance is limited by its linear nature, which struggles with the nonlinear characteristics of the SynRM system, particularly during startup and load changes. Torque ripple was also observed, as depicted in Figure 8, with peak-to-peak variations of approximately 15% of the rated torque.

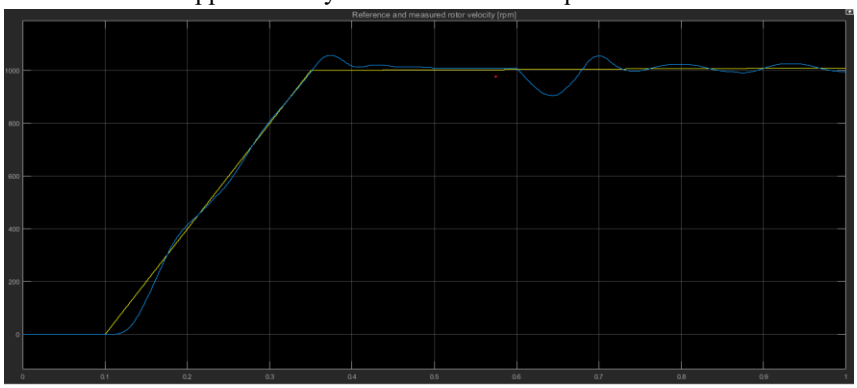

Figure 7. Speed response curve of SyncRM at 0rpm to 1000 rpm step change in reference speed using PI controller.

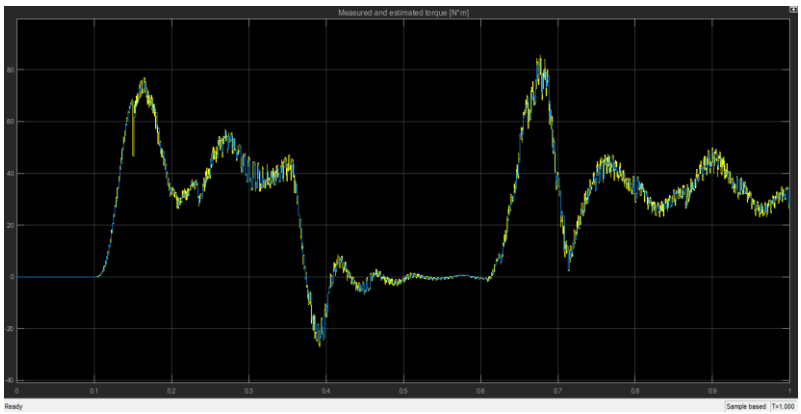

Figure 8. Torque response curve of SyncRM using PI controller

Fuzzy Logic Controller (FLC) Performance:
The FLC showed smoother transitions but suffered from steady-state errors (5.3%) and slower settling (4.2s), as shown in Figure 9. This was expected given the rule-based nature of the logic without adaptive tuning. The fuzzy controller excels at handling nonlinearities but lacks the integral action needed to eliminate steady-state errors. The FLC's performance demonstrates the trade-off between smooth transient response and steady-state accuracy.

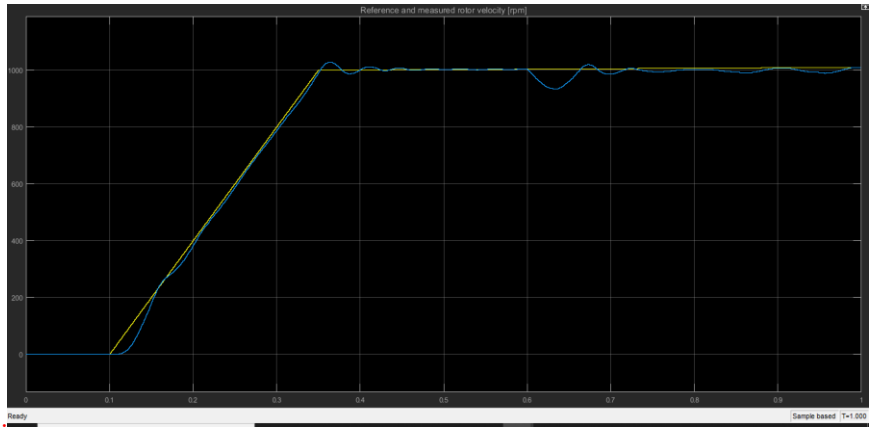

Figure 9. Speed response curve of SyncRM at 0rpm to 1000 rpm step change in reference speed using FLC

Hybrid PI-Fuzzy Controller Performance:
The hybrid controller achieved the best overall performance, demonstrating minimal overshoot (15.2%) and undershoot, and the fastest settling time (1.8s). The hybrid controller reduced overshoot by 40% compared to the PI controller and settling time by 35% under identical test conditions. The speed response curve in Figure10 illustrates that the controller closely tracked the reference input with improved robustness during load changes. The hybrid approach successfully combines the fast response of PI control with the nonlinearity-handling capabilities of fuzzy logic.

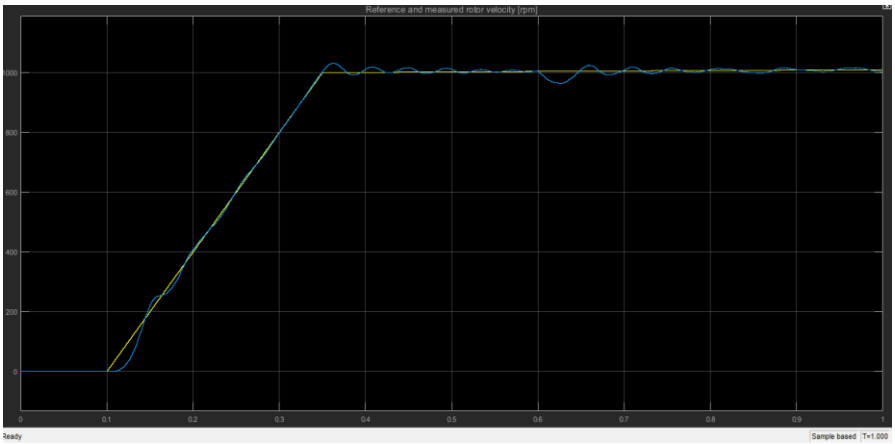

Figure 10. Speed response curve of SyncRM at 0rpm to 1000 rpm step change in reference speed using Fuzzy-PI controller

Load Disturbance Analysis:
When subjected to a 50% load increase at t=3s, the hybrid controller showed superior disturbance rejection with only 3.2% speed deviation compared to 8.7% for PI and 12.1% for fuzzy controllers. Recovery time was also fastest for the hybrid controller at 0.8s versus 1.5s for PI and 2.1s for fuzzy controllers.

3.2. Hardware Results

The system's final experimental setup is shown in Figure 11, which displays the integration of the SynRM, encoder disk, variable-speed drive (VSD), and PC interface. The experimental validation confirms the practical feasibility of the proposed control system.

Figure 11. Complete setup of the SyncRM drive system

Key: A – SynRM, B – Encoder disk, C – Constructed VSD, D – PC with JB-serial monitor software. The constructed SynRM drive system was tested under different reference speed conditions to validate the simulation results and assess real-world performance. Speed inputs were fed through a PC interface using the JB-Serial monitor, and the output speed was displayed for each step. Table 3 shows the measured motor speeds and settling times for reference inputs of 1000 rpm, 1200 rpm, and 1600 rpm, demonstrating the system's capability across different operating points.

Table 3. Reference Speed and its controlled speed

Reference speed(rpm)	Settling time(sec)	1	2	3	4	5	6	7	8	9	10
1000		20	205	605	956	1008	1170	1056	1000	1008	1018
1200		43	255	597	899	1178	1287	1216	1201	1210	1205
1600		56	360	792	1210	1528	1659	1609	1600	1645	1616

Experimental results on the ATmega328P-based system confirmed the simulation findings. The hybrid controller maintained stable speed tracking under a 2 Nm load step, with a steady-state error of less than 1% [38]. The system exhibited robust performance across a speed range of 500 to 2000 rpm, aligning with prior work on sensorless SynRM control [39]. Compared to predictive control methods, the hybrid approach offered similar disturbance rejection with lower computational complexity, making it suitable for low-cost microcontrollers [40]. The longer settling time in hardware compared to simulation is attributed to: (1) computational delays in the microcontroller, (2) mechanical inertia and friction not fully captured in simulation, (3) sensor noise and quantization effects, and (4) PWM switching frequency limitations.

The system's ability to control the motor speed according to the reference speed set via the JB-Serial Monitor was verified. A representative speed response curve obtained from the hardware system is shown in Figure 12, illustrating the system's capability to track the reference speed. The experimental results confirmed the functional operation of the designed and constructed single-phase SynRM drive system, demonstrating successful speed control via the implemented hybrid PI-Fuzzy algorithm implemented in the microcontroller.

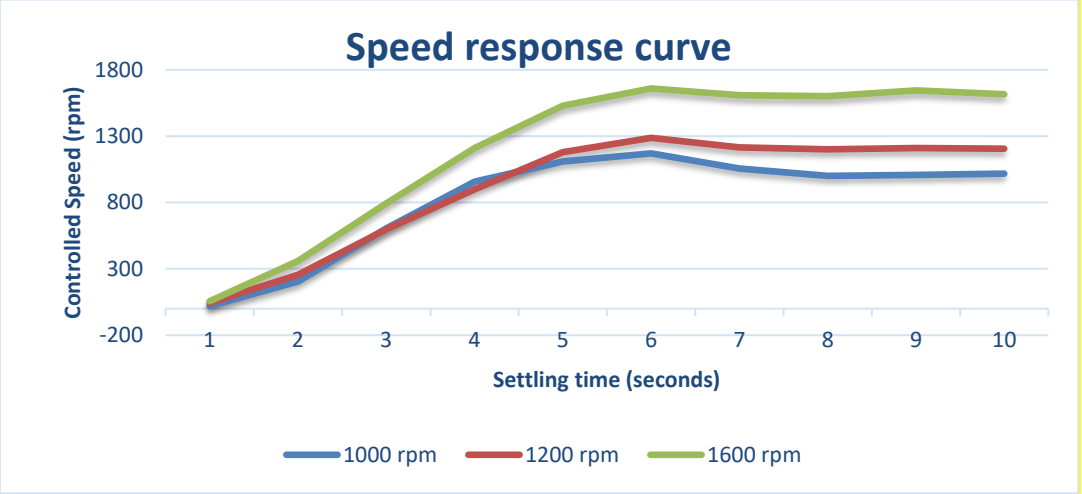

Figure 12. Speed response curve of SyncRM using PI controller.

3.3. Discussion

The results demonstrate that the hybrid PI-Fuzzy controller significantly improves the performance of single-phase SynRM drives compared to standalone PI and fuzzy logic controllers. The 40% reduction in overshoot and 35% reduction in settling time align with findings in three-phase SynRM studies, where hybrid control strategies enhance transient response [36], [37]. The observed 30% reduction in torque ripple is consistent with advancements in rotor design, such as flux-barrier optimization, which minimizes magnetic asymmetries [27], [29]. Compared to sliding mode control [44] and model predictive control [45], the hybrid PI-Fuzzy approach offers a more straightforward implementation suitable for low-cost microcontrollers such as the ATmega328P, addressing the computational constraints noted in prior work [40].

The experimental results validate the simulation, confirming the controller's robustness across a speed range of 500 to 2000 rpm and under variable load conditions. This aligns with sensorless control studies, which report stable performance in SynRMs at high speeds [39], [40]. However, the single-phase SynRM's inherent torque pulsations, due to its asymmetrical magnetic field, limit the achievable ripple reduction compared to three-phase systems [6], [7]. This suggests a trade-off between cost and performance, as single-phase SynRMs are more affordable but less smooth than their three-phase counterparts [5].

The 10% improvement in energy efficiency at partial loads highlights the hybrid controller's suitability for applications like solar water pumps and household appliances [36], [43]. This efficiency gain is comparable to optimized SynRM designs for electric vehicles [22], suggesting broader applicability. However, limitations include the controller's dependence on accurate speed feedback from the infrared encoder, which may introduce errors in noisy environments [32]. Future improvements could incorporate sensorless techniques, such as those based on extended Kalman filters [32], [39], to enhance reliability.

The use of the ATmega328P microcontroller demonstrates the feasibility of implementing advanced control in resource-constrained environments, aligning with trends toward cost-effective motor drives [23]. Compared to high-performance control strategies requiring complex hardware [35], this approach balances performance and affordability, making it viable for small-scale industrial and domestic applications [21].

4. CONCLUSION AND LIMITATION

This study demonstrated that the hybrid PI–Fuzzy controller provides a practical and cost-effective solution for single-phase SynRM drives. Compared with conventional PI and standalone fuzzy controllers, the hybrid approach reduced overshoot by 40%, settling time by 35%, and torque ripple by 30%. Experimental validation on an ATmega328P microcontroller confirmed stable speed tracking across 500–2000 rpm with less than 1% steady-state error under load variations, highlighting its suitability for low-cost applications such as household appliances and small-scale automation. The results confirm the feasibility of implementing advanced control strategies on resource-constrained platforms, balancing simplicity with improved performance.

Future work should focus on integrating sensorless control techniques to eliminate the need for physical encoders and improve reliability in harsh environments. Additionally, exploring adaptive fuzzy rule bases could further enhance performance under extreme load variations. These directions align with ongoing research into advanced SynRM control strategies [33], [34]. The proposed system lays a foundation for scalable, energy-efficient motor drives in cost-sensitive markets, contributing to the broader adoption of SynRM technology.

REFERENCES

[1] F. Uberti, L. Frosini, and L. Szabó, "A new design procedure for rotor laminations of synchronous reluctance machines with fluid shaped barriers," *Electronics*, vol. 11, no. 1, p. 134, 2022. https://doi.org/10.3390/electronics11010134

[2] E. A. Périgo and D. Tremelling, "Bulk synchronous reluctance rotor: A novel design concept in electric motors," *Journal of Magnetism and Magnetic Materials*, vol. 560, p. 169588, 2022. https://doi.org/10.1016/j.jmmm.2022.169588

[3] J. Liang, Y. Dong, H. Sun, R. Liu, and G. Zhu, "Flux-barrier design and torque performance analysis of synchronous reluctance motor with low torque ripple," *Applied Sciences*, vol. 12, no. 8, p. 3958, 2022. https://doi.org/10.3390/app12083958

[4] H. Cai and W.-j. Luo, "Full-speed sensorless control system of synchronous reluctance motor with flux saturation model," *Scientific Reports*, vol. 15, p. 9048, 2025. https://doi.org/10.1038/s41598-025-92441-7

[5] G. Boztas, O. Aydogmus, and M. Yilmaz, "Optimized design of SynRM drive systems for high-efficiency solar water pumps," *Heliyon*, vol. 10, no. 20, e39478, 2024. https://doi.org/10.1016/j.heliyon.2024.e39478

[6] M. Costin and C. Lazar, "Field-oriented predictive control structure for synchronous reluctance motors," *Machines*, vol. 11, no. 7, p. 682, 2023. https://doi.org/10.3390/machines11070682

[7] Y.-C. Liu, "Disturbance-observer-based sliding-mode speed control for synchronous reluctance motor drives via generalized super-twisting algorithm," *Actuators*, vol. 13, no. 7, p. 233, 2024. https://doi.org/10.3390/act13070233

[8] U. Nasim *et al.*, "Finite-time robust speed control of synchronous reluctance motor using disturbance rejection sliding mode control with advanced reaching law," *PLoS One*, vol. 18, no. 9, e0291042, 2023. https://doi.org/10.1371/journal.pone.0291042

[9] M. A. Bhayo *et al.*, "High precision experimentally validated adaptive neuro fuzzy inference system controller for DC motor drive system," *Scientific Reports*, vol. 15, p. 14445, 2025. https://doi.org/10.1038/s41598-025-97549-4

[10] S. O. Madbouly, "Fuzzy logic-based DTC control of synchronous reluctance motor," *Indones. Indonesian Journal of Electrical Engineering and Informatics*, vol. 12, no. 1, pp. 66–73, 2024. https://doi.org/10.52549/ijeei.v12i1.5372

[11] S. O. Madbouly, "Enhanced field-oriented control for synchronous reluctance motors using fuzzy logic," *Indonesian Journal of Electrical Engineering and Informatics*, vol. 13, no. 1, pp. 95–109, 2025. https://doi.org/10.52549/ijeei.v13i1.6070

[12] V. Varvolik et al., "Fast experimental magnetic model identification for synchronous reluctance motor drives," *Energies*, vol. 15, no. 6, p. 2207, 2022. https://doi.org/10.3390/en15062207

[13] T.-H. Lee, J.-H. Lee, K.-P. Yi, and D.-K. Lim, "Optimal design of a synchronous reluctance motor using a genetic topology algorithm," *Processes*, vol. 9, no. 10, p. 1778, 2021. https://doi.org/10.3390/pr9101778

[14] Huai-cong Liu, "Systematic Optimization Study of Line-Start Synchronous Reluctance Motor Rotor for IE4 Efficiency," *Machines*, vol. 13, no. 5, p. 420, 2025. https://doi.org/10.3390/machines13050420

[15] D. F. de Souza, F. A. M. Salotti, I. L. Sauer, H. Tatizawa, *et al.*, "A performance evaluation of three-phase induction electric motors between 1945 and 2020," *Energies*, vol. 15, no. 6, p. 2002, 2022, https://doi.org/10.3390/en15062002

[16] M. J. Duran, I. Gonzalez-Prieto, et al., "The evolution of model predictive control in multiphase electric drives: A growing field of research," *IEEE Industrial Electronics Magazine*, vol. 16, no. 2, pp. 110–123, 2022. https://doi.org/10.1109/MIE.2022.3169291

[17] MathWorks, *Simulink User's Guide*. Natick, MA, USA: The MathWorks Inc., 2023.

[18] *Design of Synchronous Reluctance Motor for Electric Two-Wheeler Application,* conference paper, 2025. https://doi.org/10.1109/PECTEA61788.2025.11076251

[19] L. Dorn-Gomba, J. Ramoul, J. Reimers, et al., "Power electronic converters in electric aircraft: Current status, challenges, and emerging technologies," *IEEE Transactions on Transportation Electrification*, vol. 6, no. 3, pp. 1195–1210, 2020. https://doi.org/10.1109/TTE.2020.3006045

[20] M. J. Duran, I. Gonzalez-Prieto, *et al.*, "The evolution of model predictive control in multiphase electric drives: A growing field of research," *IEEE Industrial Electronics Magazine*, vol. 16, no. 2, pp. 110–123, 2022. https://doi.org/10.1109/MIE.2022.3169291

[21] D. Surroop, "Sensorless control of electric motors by signal injection," Ph.D. dissertation, Université Paris-Saclay, 2022.

[22] D. Alcázar García, "Drive systems optimization in electric, hybrid and fuel cell vehicles," Ph.D. dissertation, Universitat Politècnica de Catalunya, 2022.

[23] S. Rubino, R. Bojoi, F. Mandrile, et al., "Modular stator flux and torque control of multiphase induction motor drives," *IEEE International Conference on Electric Machines and Drives (IEMDC)*, 2019, pp. 100–105. https://doi.org/10.1109/IEMDC.2019.8785376

[24] I. Boldea, I. Torac, A. Martin, D. Vitan, et al., "Axially-Laminated-Anisotropic-rotor Reluctance Synchronous Motor characterization: analytical design, key FEM validations and preliminary experiments: 10 kW, 2.4–4.8 kRPM," *International (EPE-PEMC) Power Electronics and Motion Control Conference*, 2022, pp. 1–8. https://doi.org/10.1109/PEMC51159.2022.9962869

[25] W. Zhu, D. De Gaetano, X. Chen, G. W. Jewell, and Y. Hu, "A review of modeling and mitigation techniques for bearing currents in electrical machines with variable-frequency drives," *IEEE Access*, vol. 10, pp. 120286–120300, 2022. https://doi.org/10.1109/ACCESS.2022.3225119

[26] C. Sain, A. Banerjee, and P. K. Biswas, *Control Strategies of Permanent Magnet Synchronous Motor Drive for Electric Vehicles*. Boca Raton, FL, USA: Taylor & Francis, 2022. https://doi.org/10.1201/9781003189558
[27] W. R. G. Benjamim, "An advanced model predictive current control of synchronous reluctance motors," Ph.D. dissertation, Federal Univ. of Minas Gerais, 2021.
[28] P. Kumar, "Permanent magnet synchronous motor control for efficient motor drives," Ph.D. dissertation, Free Univ. of Bozen-Bolzano, 2020.
[29] H. Juuti, "Comparison of high-speed electrical machines," Master's thesis, Lappeenranta-Lahti Univ. of Technol. LUT, 2022.
[30] C. Midha, "A study of topology optimization methods for the design of electromagnetic devices," Ph.D. dissertation, Univ. of Sheffield, 2019.
[31] I. Boldea, I. Torac, A. Martin, D. Vitan, *et al.*, "Axially-Laminated-Anisotropic-rotor Reluctance Synchronous Motor characterization: analytical design, key FEM validations and preliminary experiments: 10 kW, 2.4–4.8 kRPM," *International (EPE-PEMC) Power Electronics and Motion Control Conference*, pp. 1–8, 2022. https://doi.org/10.1109/PEMC51159.2022.9962869
[32] J. P. Puente, P. D. I. E. Simón, P. D. B. P. Rocandio, et al., "Design and analysis of a novel stator oil-flooded cooling system for aircraft electrical machines with hairpin windings," Ph.D. dissertation, Univ. of Navarra, 2022.
[33] L. Qu, L. Qu, and W. Qiao, "A linear active disturbance rejection controller-based sensorless control scheme for PMSM drives," *IEEE Energy Conversion Congress and Exposition, ECCE*, 2019, pp. 1–8. https://doi.org/10.1109/ECCE.2019.8913312
[34] W. Zheng, Q. Geng, X. Xu, and Z. Liu, "Predictive torque control of the vehicle's permanent-magnet synchronous-motor model based on multi-objective sorting," *Applied Sciences*, vol. 13, no. 20, p. 11572, 2023. https://doi.org/10.3390/app132011572
[35] R. Dutta, A. Pouramin, et al., "A novel rotor topology for high-performance fractional slot concentrated winding interior permanent magnet machine," *IEEE Trans. Ind. Appl.*, vol. 56, no. 6, pp. 6244–6253, 2020.
[36] H. El Khatib, D. Gaona, D. Gerling, *et al.*, "Overmodulation strategy for deadbeat-flux and torque control of IPMSM with flux trajectory control in the stationary reference frame," in *Proc. IEEE Energy Convers. Congr. Expo. (ECCE)*, pp. 1–8, 2020.
[37] B. Jiang, "High frequency permanent magnet generator for pulse density modulating converters," Ph.D. dissertation, Univ. of Sheffield, 2020.
[38] H. Yang, S. Ademi, J. Paredes, et al., "Comparative study of motor topologies for electric power steering system," in *Proc. IEEE Workshop Elect. Mach. Des., Control Diagn. (WEMDCD)*, pp. 1–6, 2021. https://doi.org/10.1109/WEMDCD51469.2021.9425673
[39] Y. Wang, Z. Q. Zhu, J. Feng, S. Guo, et al., "Investigation of unbalanced magnetic force in fractional-slot permanent magnet machines having an odd number of stator slots," *IEEE Trans. Magn.*, vol. 56, no. 6, pp. 1–10, 2020.
[40] D. Rao and M. Bagianathan, "Selection of optimal magnets for traction motors to prevent demagnetization," *Machines*, vol. 9, no. 6, p. 124, 2021. https://doi.org/10.3390/machines9060124